JHG-18-688 R2

ARTICLE

Identification of a homozygous frameshift variant in *RFLNA* in a patient with a typical phenotype of spondylocarpotarsal synostosis syndrome

Hitomi Shimizu[1,2], Satoshi Watanabe[1], Akira Kinoshita[2], Hiroyuki Mishima[2], Gen Nishimura[3], Hiroyuki Moriuchi[1], Koh-ichiro Yoshiura[2], and Sumito Dateki[1*]

[1] Department of Pediatrics, Nagasaki University Graduate School of Biomedical Sciences, Nagasaki, Japan

[2] Department of Human Genetics, Nagasaki University Graduate School of Biomedical Sciences, Nagasaki, Japan

[3] Center for Intractable Disease, Saitama Medical University Hospital, Saitama, Japan

Running title: A patient with a homozygous *RFLNA* mutation

Conflicts of interest: The authors declare no conflicts of interest in association with the present study.

This work was supported by a grant for the Initiative on Rare and Undiagnosed Diseases in Pediatrics (no. 18gk0110012h0101) from the Japan Agency for Medical Research and Development (AMED), Tokyo, Japan.

[*]**Correspondence to**

Sumito Dateki, M.D.

Department of Pediatrics, Nagasaki University Graduate School of Biomedical Sciences

Address: 1-7-1 Sakamoto, Nagasaki, 852-8501 Japan

E-mail: sdateki1@nagasaki-u.ac.jp

Phone: +81-95-819-7298, FAX: +81-95-819-7301

Abstract

Spondylocarpotarsal synostosis syndrome, a rare syndromic skeletal disorder characterized by disrupted vertebral segmentation with vertebral fusion, scoliosis, short stature and carpal/tarsal synostosis, has been associated with biallelic truncating mutations in the filamin B gene or monoallelic mutations in the myosin heavy chain 3 gene. We herein report the case of a patient with a typical phenotype of spondylocarpotarsal synostosis syndrome who had a homozygous frameshift mutation in the refilin A gene (*RFLNA)* [c.241delC, p.(Leu81Cysfs*111)], which encodes one of the filamin binding proteins. Refilins, filamins, and myosins play critical roles in forming perinuclear actin caps, which change the nuclear morphology during cell migration and differentiation. The present study implies that *RFLNA* is an additional causative gene for spondylocarpotarsal synostosis syndrome in humans and a defect in forming actin bundles and perinuclear actin caps may be a critical mechanism for the development of spondylocarpotarsal synostosis syndrome.

Introduction

Spondylocarpotarsal synostosis syndrome (SCT) (OMIM #272460) is characterized by disrupted vertebral segmentation with vertebral fusion, scoliosis, short stature, and carpal/tarsal synostosis. Mutations in filamin B (*FLNB*) (NM_001457) and myosin heavy chain 3 (*MYH3*) (NM_002470) have been identified in patients with autosomal recessive and autosomal dominant SCT, respectively [1-3].

Mutations in *FLNB* cause five distinct skeletal diseases (SCT, Larsen syndrome, atelosteogenesis type I, atelosteogenesis type III, and boomerang dysplasia). Among these, only SCT is inherited in an autosomal recessive manner; the others are inherited in an autosomal dominant manner [4]. *FLNB* mutations have been reported in at least 16 families with SCT [5], all of whom showed either nonsense or frameshift biallelic mutations predicted to induce premature translation termination or consecutive changes in amino acid sequences, indicating that conditions brought about by severe FLNB defects are associated with phenotypes of SCT [1, 2, 4].

Filamins are dimeric actin binding proteins [6]. Refilin A (RFLNA) and Refilin B (RFLNB) (also known as FAM101A and FAM101B, respectively) have been identified as vertebrate-specific short-lived filamin-binding proteins. Under TGF-β stimulation, filamins bind to RFLNs and transform their connecting actins into parallel bundle structures that accumulate each other to form perinuclear actin caps (Fig. 1a, b, c). A series of the processes above is important for cell migration and differentiation leading to endochondral ossification and skeletal development [6, 7].

We herein report the case of a Japanese boy with a typical phenotype of SCT who had a homozygous frameshift variant in *RFLNA* (NM_181709). We propose that *RFLNA* is an additional causative gene for SCT in humans.

Materials and methods

Case report

The patient was born at 34 weeks of gestation. At birth, his length was 43 cm (-0.7 SD) and his weight was 2.35 kg (+0.3 SD). An X-ray examination at the time of birth showed seemingly normal segmented vertebrae. At 1 year and 2 months of age, the patient was referred to us because of severe short stature. His height was 67.2 cm (-3.7 SD), weight 7.8 kg (-2.2 SD), and occipital frontal circumference 47 cm (+1.1 SD). He also had mild facial dysmorphic features with frontal bossing and anteverted nares. A skeletal survey showed spondylar fusion mainly affecting the posterior neural arches and to a lesser degree the vertebral bodies with mild scoliosis and carpo-tarsal synostosis (fusion of the capitate and hamate and probably that of the cuboid and lateral cuneiform) (Fig. 2). He was diagnosed with SCT based on his characteristic skeletal features, severe short stature, and progressive clinical course. At the last examination at 2 years and 3 months of age, he was 72.4 cm tall (-4.3SD). His motor and mental development was normal. The patient's parents were non-consanguineous. The patient's father and elder brother were phenotypically normal, while his mother showed short stature (147 cm, –2.2 SD) without dysmorphic facial features or scoliosis.

Whole exome sequencing

The family underwent trio whole-exome sequencing (WES). Genomic DNA extracted from peripheral blood leukocytes was captured using Agilent SureSelect Exome Target Enrichment System v6 (Agilent Technologies, Santa Clara, CA, USA) and sequenced on a HiSeq^{TM} 2500 (Illumina, San Diego, CA, USA) with 150 bp paired-end reads. Fastq format files were generated and aligned on the hg19/GRCh37 human reference genome sequence using the Novoalign software program (Novocraft Technologies,

Kuala Lumpur, Malaysia). The Genome Analysis Toolkit (GAKT HaplotypeCaller) was used for variant calling and consequently implemented in an in-house workflow management tool [8,9]. Single nucleotide variations and insertions/deletions were annotated using the ANNOVAR software program [10]. Then, rare and deleterious variants were filtered using a previously described method [11]. Based on this pedigree, autosomal dominant, recessive, and X-linked recessive models of inheritance were assumed for the analysis. This study was approved by the Institutional Review Board Committee at Nagasaki University Graduate School of Biomedical Sciences.

PCR-based expression analyses of *RFLNA*

Total RNA was extracted from lymphoblastoid cell lines derived from the proband with the *RFLNA* mutation and the parents using the NucleoSpin RNA Plus kit (Takara, Shiga, Japan). RNA (2.0 μg) was reverse transcribed using the PrimeScript™ II 1st strand cDNA Synthesis Kit (Takara). The obtained cDNA and control genome DNA were amplified by PCR with primers for exon 2 (5'-GCATCAAGGTGAACCCGGA-3') and the 3' untranslated region in exon 3 (5'- GGCTGTTCTCTGCTTCAAGG-3') for the *RFLNA* gene, as well as those for exon 5 (5'- GAACAAGGTTAAAGCCGAGCC-3') and exon 6 (5'- GTGGCAGATTGACTCCTACCA-3') for the *PGK1* gene (NM_000291), which was utilized as an internal control. Subsequently, the PCR products were subjected to direct sequencing.

Results

Trio WES revealed a homozygous frameshift variant in the last exon 3 of the *RFLNA* gene in the patient (chr12:124 798 904C>- [GRCh37/hg19]; c.241delC [NM_181709]) (Fig. 3a). The parents were heterozygous for the variant. The mutational analyses were

not done for the phenotypically normal elder brother. This variant is predicted to cause a frameshift at codon 81 for *RFLNA*, skip the initial 136th termination codon, and result in the production of an additional 110 aberrant amino acids (p.(Leu81Cysfs*111)) (NP_859060). PCR-based expression and sequence analyses using cDNA derived from lymphoblastoid cell lines showed that the mutant allele was expressed in the patient (Fig. 3b), and the mutant and the wild type alleles were expressed in the parents with the heterozygous *RFLNA* variant (data not shown; Fig. 3b) [6]. The variant in *RFLNA* has not been registered in the following databases: 1000G (www.1000genomes.org), Exome Aggregation Consortium (ExAC; http://exac.broadinstitute.org/) and Integrative Japanese Genome Variation Database (3.5KJPN; https://ijgvd.megabank.tohoku.ac.jp/).

In addition, a rare heterozygous missense variant in the *FLNB* gene (chr3:58 121 852C>G [GRCh37/hg19]; c.4818C>G [NM_001457.3], p.Ile1606Met [NP_001448.2] [rs774972522]) was identified in the patient and the mother. The father had no deleterious variants in *FLNB*. The minor allele frequency of the c.4818C>G in *FLNB* variant in the general population was reported to be 0.27% in the 3.5 KJPN database. *In silico* analyses performed using PolyPhen-2 (http://genetics.bwh.harvard.edu/pph2/) and MutationTaster (http://www.mutationtaster.org) predicted that this rare variant would be pathogenic. The expression analyses of the proband revealed a biallelic expression of *FLNB* without abnormal splicing variants or exonic deletions (data not shown).

There were no mutations in *MYH3*, *RFLNB*, or other genes known to be related to vertebral segmentation formation [12].

Discussion

We identified a rare maternally derived missense *FLNB* variant (c.4818C>G,

142 p.Ile1606Met) in the present patient with a typical phenotype of SCT. While SCT is
143 caused by biallelic truncating mutations in *FLNB* [1, 2, 4], the expression analyses in
144 this study showed a biallelic expression of *FLNB,* including normal transcripts of *FLNB*
145 that originated from the paternal allele in the patient, indicating that the patient is
146 certainly heterozygous for the *FLNB* variant. Furthermore, the *FLNB* variant has been
147 identified among the general Japanese population. In addition, the mother with the same
148 variant does not show the typical SCT phenotype. Collectively, the present data argue
149 against any pathological role of the missense variant in the development of SCT,
150 although the possibility that the variant might function as a susceptibility factor for the
151 development of SCT or short stature remains tenable. Thus, a mutation(s) in a new,
152 undiscovered gene(s) may be responsible for SCT in the patient.
153 In this regard, we identified a novel homozygous frameshift mutation in *RFLNA*
154 in the patient, and propose the homozygous mutation of *RFLNA* as another genetic
155 cause of SCT, based on the following findings. First, although mice with the single
156 knockout of either *Rflna* or *Rflnb* (also known as *Cfm2* and *Cfm1*, respectively)
157 displayed wild-type phenotypes, double knockout mice manifested progressive scoliosis,
158 kyphosis, vertebral fusions, intervertebral disc defects, and growth retardation [13]. The
159 above phenotype is similar to that of *Flnb*-deficient mice and of human SCT patients,
160 indicating that defects of RFLN families may lead to the phenotype of SCT in humans
161 [1, 2, 4]. At this point, there is a phenotypic difference between *Rflna* single knockout
162 mice and our patient with a homozygous *RFLNA* mutation. This may be associated with
163 the difference of their genetic background and/or gene expression pattern [14]. Second,
164 only a few heterozygous truncating variants and no homozygous null variants in *RFLNA*
165 have been registered in ExAC database, implying that biallelic *RFLNA* mutations result

in some pathogenic effects in humans. Third, *Rflna* is expressed in the vertebral primordia, vertebral bodies and carpal bones in embryonic mice and the expression is increased in prehypertrophic chondrocytes, implying the positive role of RFLNA in vertebral and carpal/tarsal bone development [15]. Fourth, a significantly decreased expression level of *RFLNA* has been observed in primary osteoblasts derived from the spinal vertebrae in patients with adolescent idiopathic scoliosis [16]. This result indicates that RFLNA has an important role in the normal development and growth of the vertebral column. Finally, the variant is predicted to retain the filamin binding domains (FBDs) 1 and 2 but lose FBD3 and FBD4 (Fig. 3c) and thereby hardly form parallel actin bundles. Thus, the variant is likely a loss-of-function mutation, although the abnormal amino acid extension may result in the acquisition of some neomorphic functions. Indeed, primary rib chondrocytes from *Rflna* and *Rflnb* double knockout mice formed fewer actin bundles [13]. A biallelic *Flnb* defect is also predicted to affect the parallel actin bundle formation. In addition, *MYH3* mutations have been reported to alter TGF-β canonical signaling [3]. Thus, a defect in forming actin bundles and perinuclear actin caps may be a critical mechanism responsible for the development of SCT.

In conclusion, we propose, for the first time, an association between a homozygous mutation of *RFLNA* and SCT. Further studies and the accumulation of additional cases with *RFLNA* mutations are needed to clarify the pathogenic significance of *RFLNA* mutations.

Conflicts of interest

The authors declare no conflicts of interest in association with the present study.

Acknowledgements

We thank the family who participated in this study. We also thank Yasuko Noguchi and Chisa Koga for their technical assistance. This work was supported by a grant for the Initiative on Rare and Undiagnosed Diseases in Pediatrics (no. 18gk0110012h0101) from the Japan Agency for Medical Research and Development (AMED), Tokyo, Japan.

References

1. Krakow D, Robertson SP, King LM, Morgan T, Sebald ET, Bertolotto C, et al. Mutations in the gene encoding filamin B disrupt vertebral segmentation, joint formation and skeletogenesis. Nat Genet. 2004;36:405–10.

2. Farrington-Rock C, Kirilova V, Dillard-Telm L, Borowsky AD, Chalk S, Rock MJ, et al. Disruption of the Flnb gene in mice phenocopies the human disease spondylocarpotarsal synostosis syndrome. Hum Mol Genet. 2009;17:631–41.

3. Zieba J, Zhang W, Chong JX, Forlenza KN, Martin JH, Heard K, et al. A postnatal role for embryonic myosin revealed by MYH3 mutations that alter TGFβ signaling and cause autosomal dominant spondylocarpotarsal synostosis. Sci Rep. 2017;7:41803.

4. Xu Q, Wu N, Cui L, Wu Z, Qiu G. Filamin B: The next hotspot in skeletal research? J Genet Genomics. 2017;44:335–42

5. Salian S, Shukla A, Shah H, Bhat SN, Bhat VR, Nampoothiri S. et al. Seven additional families with spondylocarpotarsal synostosis syndrome with novel biallelic deleterious variants in FLNB. Clin Genet. 2018;94:159-64

6. Baudier J, Jenkins ZA, Robertson SP. The filamin-B-refilin axis - spatiotemporal regulators of the actin-cytoskeleton in development and disease. J Cell Sci. 2018;13:131.

7. Khatau SB, Hale CM, Stewart-Hutchinson PJ, Patel MS, Stewart CL, Searson PC, et

217 al. A perinuclear actin cap regulates nuclear shape. Proc Natl Acad Sci U S A.
218 2009;10:19017-22.

219 8. McKenna A, Hanna M, Banks E, Sivachenko A, Cibulskis K, Kernytsky A. et al.
220 The Genome Analysis Toolkit: a MapReduce framework for analyzing next-
221 generation DNA sequencing data. Genome Res. 2010;20:1297–303.

222 9. Mishima H, Sasaki K, Tanaka M, Tatebe O, Yoshiura K. Agile parallel
223 bioinformatics workflow management using Pwrake. BMC Res Notes. 2011;4:331–
224 8.

225 10. Wang K, Li M, Hakonarson H. ANNOVAR: functional annotation of genetic
226 variants from high-throughput sequencing data. Nucleic Acids Res. 2010;38:e164.

227 11. Morimoto Y, Shimada-Sugimoto M, Otowa T, Yoshida S, Kinoshita A, Mishima H,
228 et al. Whole-exome sequencing and gene-based rare variant association tests suggest
229 that PLA2G4E might be a risk gene for panic disorder. Transl Psychiatry. 2018;8:41

230 12. Gibb S, Maroto M, Dale JK. The segmentation clock mechanism moves up a notch.
231 Trends Cell Biol. 2010;20:593–600.

232 13. Mizuhashi K, Kanamoto T, Moriishi T, Muranishi Y, Miyazaki T, Terada K, et al.
233 Filamin-interacting proteins, Cfm1 and Cfm2, are essential for the formation of
234 cartilaginous skeletal elements. Hum Mol Genet. 2014;23:2953–67.

235 14. Liao BY, Zhang J. Null mutations in human and mouse orthologs frequently result
236 in different phenotypes. Proc Natl Acad Sci U S A. 2008:105:6987–92.

15. Gay O, Gilquin B, Nakamura F, Jenkins ZA, McCartney R, Krakow D, et al. RefilinB (FAM101B) targets filamin A to organize perinuclear actin networks and regulates nuclear shape. Proc Natl Acad Sci U S A. 2011;12:11464–9.

16. Fendri K, Patten SA, Kaufman GN, Zaouter C, Parent S, Grimard G, et al. Microarray expression profiling identifies genes with altered expression in Adolescent Idiopathic Scoliosis. Eur Spine J. 2013;22:1300–11.

Titles and legends to figures

Fig. 1. A schematic illustration of filamins and the formation of parallel actin bundles and perinuclear actin caps.

(a) The structure of a monomeric chain of filamins. Filamin contains two calponin homology domains (CH1 and CH2) that have actin binding affinity followed by 24 β-pleated sheet immunoglobulin (Ig)-like repeats (ellipses). The repeats are interrupted by two flexible hinge regions (H1 and H2) that allow filamins for structural flexibility. The Ig-like repeats contain another actin-binding domain (ABD), two RFLNs binding domains, and a C-terminal domain that contains a mechanosensor region (MSR) [5]. (b) Schematic illustration of a vertebrate filamin dimer (left) and formation of parallel actin bundles (right). Under the TGF-β stimulations, filamins bind to RFLNs and transform their connecting actin into a parallel bundle structure. During this process, MSRs release their holding mediators like SMADs to induce downstream signals. (c) The parallel actin bundles accumulate and produce perinuclear actin caps. These actin dynamics are necessary for cellular migration and differentiation. These figures are modified from those of Baudier et al [6] and Khatau et al [7].

Fig. 2. Radiological examinations of the patient.

(a) Dorsal (left, middle) and ventral (right) views of spinal three-dimensional computed tomography at 1 year 7 months of age show scoliosis, vertebral fusions and dysraphisms (white arrows). (b) Carpal (left) and tarsal (right) synostoses at 1 year 2 months of age (white arrows).

Fig. 3. The *RFLNA* variant of the proband.

(a) Electrochromatograms delineating a homozygous frameshift *RFLNA* variant

(c.241delC, p.(Leu81Cysfs*111)) (NM_181709, NP_859060.3) in the proband. (b) PCR-based expression analyses for *RFLNA* (35 cycles) (upper) and the sequencing analysis (lower). *PGK1* has been used as an internal control (20 cycles). The mutant *RFLNA* is expressed in lymphoblastoid cell lines derived from the proband as well as the parents with the heterozygous *RFLNA* mutation. NC, negative control. (c) The position of the *RFLNA* variant and the estimated structure of the mutant protein. This variant is predicted to skip the initial termination, and result in the production of an additional 110 aberrant amino acids (a gray box). This mutated protein is predicted to retain the filamin binding domains (FBDs) 1 and 2 but lose the FBD3 and FBD4 (blue boxes).

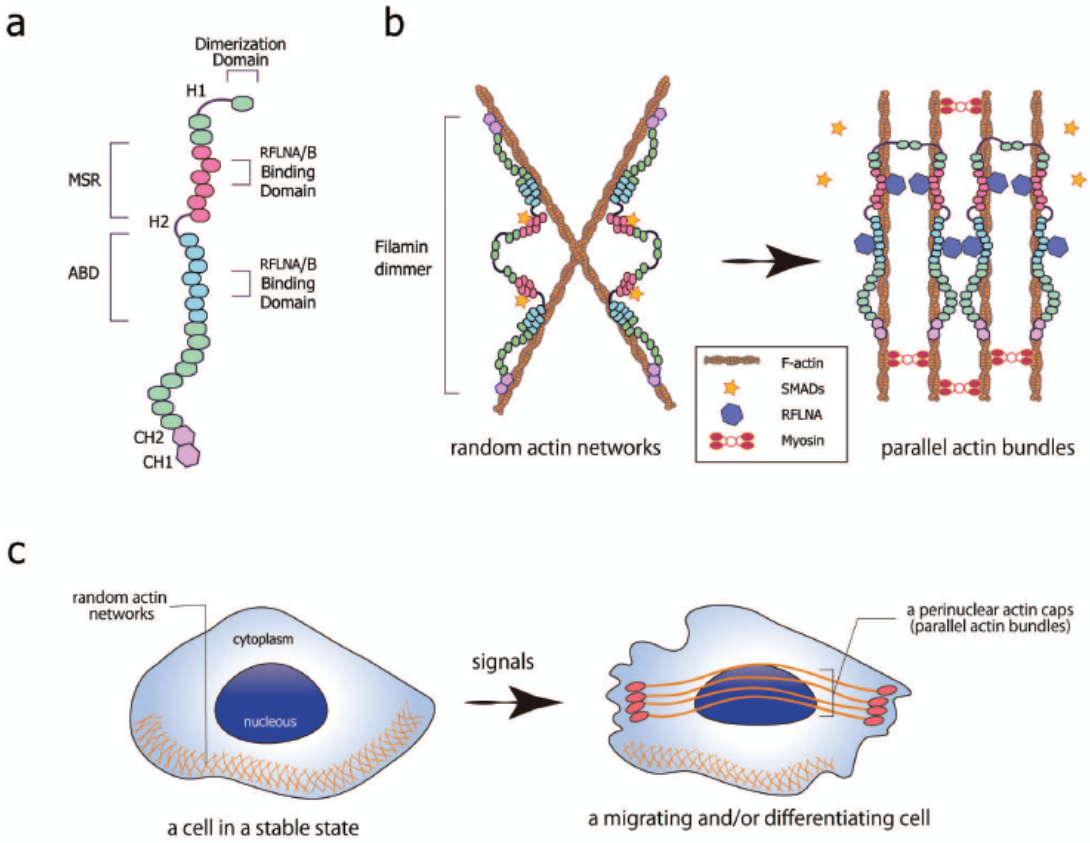
a
Dimerization Domain
H1
MSR
RFLNA/B Binding Domain
H2
ABD
RFLNA/B Binding Domain
CH2
CH1
b
Filamin dimmer
random actin networks
F-actin
SMADs
RFLNA
Myosin
parallel actin bundles
c
random actin networks
cytoplasm
nucleous
a cell in a stable state
signals
a perinuclear actin caps (parallel actin bundles)
a migrating and/or differentiating cell

Fig. 1

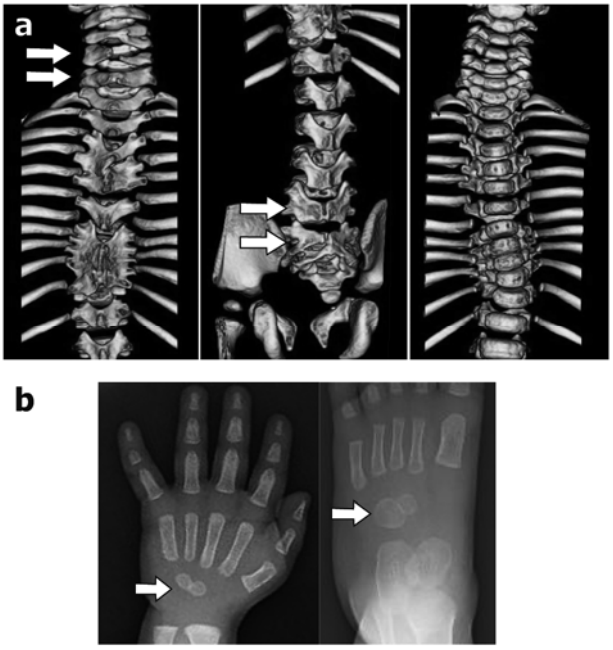

Fig. 2

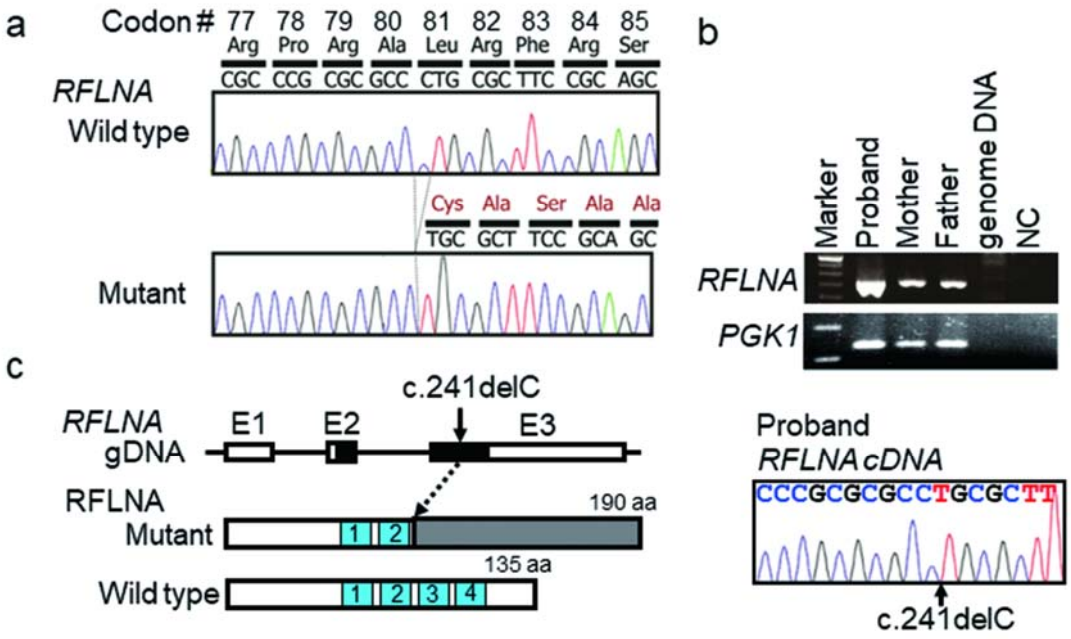
a
Codon # 77 78 79 80 81 82 83 84 85
Arg Pro Arg Ala Leu Arg Phe Arg Ser
CGC CCG CGC GCC CTG CGC TTC CGC AGC
RFLNA
Wild type
Cys Ala Ser Ala Ala
TGC GCT TCC GCA GC
Mutant
b
Marker
Proband
Mother
Father
genome DNA
NC
RFLNA
PGK1
c
c.241delC
RFLNA
gDNA
E1
E2
E3
RFLNA
Mutant
190 aa
1 2
135 aa
Wild type
1 2 3 4
Proband
RFLNA cDNA
CCCGCGCGCCTGCGCTT
c.241delC

Fig. 3